Toward Noninvasive Characterization of Breast Cancer and Cancer Metabolism with Diffuse Optics

David R. Busch, PhD[a,b,*], Regine Choe, PhD[c], Turgut Durduran, PhD[d], Arjun G. Yodh, PhD[b]

KEYWORDS

Diffuse optical tomography Diffuse optical spectroscopy Metabolic imaging Blood flow Breast cancer Neoadjuvant chemotherapy

KEY POINTS

- Diffuse optical spectroscopies provide noninvasive, nonionizing, serial measurements of tissue blood flow, oxygenation, and concentration.
- These physiologic parameters provide a window into tissue metabolism without necessitating the use of ionizing radiation or transport to imaging suites.
- Current clinical investigations of diffuse optical mammography include applications of diffuse optical tomography and monitoring to neoadjuvant chemotherapy, contrast agent discovery, computer-aided detection, and measurement of breast oxygen metabolism.
- Diffuse optical measurements hold significant promise for commercialization and clinical integration.

A.G.Y. gratefully acknowledges partial support from the National Institutes of Health through grants CA087971, NS060653, EB002109, and EB015893.
T.D. gratefully acknowledges partial support by Fundació Cellex Barcelona, Marie Curie IRG (FP7, RPTAMON), Institute de Salud Carlos III (DOM-MON, FIS), Ministerio de Ciencia e Innovación (MICINN), Ministerio de Economía y Comepetitividad, Institució CERCA (DOCNEURO, PROVAT-002-11), Generalitat de Catalunya, European Regional Development Fund (FEDER/ERDF) and LASERLAB (FP7) and Photonics4Life (FP7) consortia.
R.C. gratefully acknowledges support from the National Institutes of Health through K99/R00-CA126187.
D.R.B. gratefully acknowledges partial support from the Thrasher Research Fund and National Institutes of Health through grant NS072338.
The authors (T.D., R.C., and A.G.Y.) are coinventors in various patents about diffuse optical technologies, but they do not currently receive any royalties. There are no other conflicting financial or ethical issues to disclose.
[a] Division of Neurology, Department of Pediatrics, Children's Hospital of Philadelphia, 3615 Civic Center Boulevard, Philadelphia, PA 19104, USA; [b] Department of Physics and Astronomy, University of Pennsylvania, 3231 Walnut Street, Philadelphia, PA 19104, USA; [c] Department of Biomedical Engineering, University of Rochester, Goergen Hall, Intercampus Drive, Rochester, NY 14620, USA; [d] Medical Optics Department, ICFO - Institut de Ciències Fotòniques, Mediterranean Technology Park Avenue Carl Friedrich Gauss, 3 08860 Castelldefels (Barcelona), Spain
* Corresponding author. Division of Neurology, Department of Pediatrics, Children's Hospital of Philadelphia, Philadelphia, PA 19104.
E-mail address: drbusch@sdf.org

PET Clin 8 (2013) 345–365
http://dx.doi.org/10.1016/j.cpet.2013.04.004
1556-8598/13/$ – see front matter

Acronyms and symbols utilized in this manuscript

ACRONYMS	Description
ASL-MRI	Arterial-Spin Labeling MRI
BF	Blood Flow
CAD	Computer Aided Detection
CT (X-Ray)	Computed Tomography
DCS	Diffuse Correlation Spectroscopy
DCT	Diffuse Correlation Tomography
DOS	Diffuse Optical Spectroscopy
DOT	Diffuse Optical Tomography
DOT-CAD	Diffuse Optical Tomography - Computer Aided Detection
FDG-PET	Fluoro-deoxyglucose Positron Emission Tomography
Hb	Deoxygenated Hemoglobin Concentration
HbO_2	Oxygenated Hemoglobin Concentration
Hb_t	Total Hemoglobin Concentration
H_2O	Water Concentration
l^*	Photon Random Walk Step
l_a	Photon Absorption Length
Lipid	Lipid Concentration
M	Malignancy Parameter
μ_a	Absorption Coefficient
μ_{eff}	Overall Optical Attenuation Coefficient
$MMRO_2$	Mammary Metabolic Rate of Oxygen consumption
μ_s'	Reduced Scattering Coefficient
MRI	Magnetic Resonance Imaging
NIR	Near Infra-Red Spectral Range, 650-950 nm
NIRS	Near Infra-Red Spectroscopy (a.k.a. DOS)
OEF	Oxygen Extraction Fraction
PET	Positron Emission Tomography
$P(M)$	Probability of Malignancy
RBCs	Red Blood Cells
StO_2	Blood Oxygen Saturation
TOI	Tissue Optical Index

CONTINUOUS, NONINVASIVE MONITORING OF BLOOD VOLUME, FLOW, AND OXYGENATION

Despite major advances in diagnosis and preventive medicine, breast cancer remains among the principal causes of death in women. In the United States, for example, in 2012 approximately 230,000 new cases of breast cancer were diagnosed and roughly 40,000 died of the disease.[1] At present, clinical recommendations are focused on the early detection of cancer and risk stratification, with screening techniques ranging from breast self-examinations and clinical palpation, to serial x-ray mammographic imaging, to genetic testing. Ultrasonography and magnetic resonance (MR) imaging are frequently used in conjunction with the traditional techniques, for example, to confirm a diagnosis. Modern screening of breast cancer depends heavily on x-ray mammography, which is especially sensitive to microcalcifications. However, this structural imaging modality can suffer from low sensitivity and specificity, especially in younger women.[2]

Ultrasonographic breast imaging is highly effective in identifying classes of cysts,[3,4] but is not yet widely used for whole breast imaging. Contrast-enhanced MR imaging can be highly sensitive and some studies have reported high specificity, but it is generally applied only to high-risk populations because of its cost and limited availability.[5–7] Thus, the ideal screening modality has yet to be found, and multimodal approaches, including genetic testing, are gaining popularity.

This article is primarily concerned with the potential role of optics in clinical management of breast cancer and (possibly) screening based on the local tissue metabolism. Indeed, the enhanced glucose metabolism of cancer tissues is the basis for the success of ^{18}F-fluorodeoxyglucose (FDG) Positron Emission Tomography (PET) cancer imaging which, in breast cancer, is primarily used to identify metastases and to stage disease.[8] Measurements of the local metabolism provide insights into aggressiveness of the cancer and response to the treatments.

Significant recent research in breast cancer has been oriented toward identifying and using the potential of hemodynamic parameters such as blood flow; for example, as a means to access tissue metabolism. This reasoning is based on the fact that cancers are frequently hypermetabolic and have associated formation of angiogenic vessels, therefore local blood flow may provide a cancer contrast. Doppler-ultrasound imaging of blood flow in breast cancer has been extensively explored over the past three decades, both with and without contrast agents.[4] In MR imaging, uptake and kinetics of gadolinium chelate contrast agent provide clinicians with information on perfusion of breast cancer, and is part of the current clinical standard of care.[5] An alternative MR imaging method, arterial spin-labeling MR imaging (ASL-MRI), has proved to be very useful in probing brain blood flow without the injection of contrast agents. However, its use in the breast[9] is hampered by the low absolute blood flow in the breast tissue. Of note, none of these techniques provides information about tumor blood oxygenation; this technical limitation makes it harder to gain insights about oxidative metabolism in cancer.

Diffuse optical measurements can probe blood flow, oxygenation, and concentration, permitting calculation of tissue oxygen delivery, and perhaps offering a method to complement PET. Measurement of these important physiologic parameters has been one of the driving reasons for the continued interest in diffuse optical mammography, despite its bumpy history dating from the 1920s.[10] These methods were attractive because of their noninvasive nature, relative low cost, and other features. The photons used for clinical diffuse optical measurements are nonionizing (~1.5 eV), permitting repeated measurements without significant risk to the subjects.[11,12] Indeed, pulse-oximeters using similar wavelengths and light power are ubiquitous in hospital settings for long-term care.

Diffuse optical spectroscopy (DOS) provides a localized measurement of optical properties. In the most basic form of imaging, an array of DOS measurements can be taken and the results projected onto a two-dimensional (2D) map of tissue properties.[13,14] More sophisticated imaging strategies rely on tomographic reconstruction, in which volumetric three-dimensional (3D) maps of optical properties are reconstructed from light fluence measurements on the tissue surface. Human use of diffuse optical tomography (DOT) is most advanced in imaging of breast cancer, due in part to technical (low optical absorption and malleability of breast tissue) and logistical (public awareness of breast cancer, accessibility) factors. DOS is also sometimes referred to as near-infrared spectroscopy (NIRS).

To date, both DOS and DOT technologies have been applied to quantify the optical properties of healthy human breast tissue[15–22] and its correlation with cancer risk prediction.[23–26] Several reviews of DOT imaging of and contrast in breast cancer are also available[20,27,28]; exogenous contrast agents can also be used and are discussed later in this article. DOT has been the focus of much effort in both academic[15,29–35] and industrial[36–41] settings. More details about the DOT reconstruction process may be found in the recent review by Arridge and Schotland.[42]

Table 1 illustrates some of the broad characteristics of current imaging techniques and the niche which the authors believe diffuse optics can fill; for example, for provision of continuous metabolic measurements without the use of ionizing radiation.

One of the obvious applications of optical metabolic monitoring of tumors arises during therapy. This monitoring is of particular interest in the case of neoadjuvant chemotherapy, which is an increasingly popular treatment protocol for breast cancer. For neoadjuvant chemotherapy, drugs are administered before surgical excision[43] to reduce the tumor size and eliminate or reduce micrometastases before the surgery. **Fig. 1** delineates a potential timeline for DOS/DOT to assist in judging the efficacy of therapy planning. This sequence permits the early observation of the clinical effects of specific drug regimens which, in turn, could potentially permit early determination of the chemotherapy's effectiveness and inform clinical decisions on continuing a particular therapy. Monitoring the efficacy of neoadjuvant chemotherapy is an active area of research in clinical medicine,[44–46] including optical imaging and monitoring.[47–67]

It is not the intention of this review to cover clinical applications of diffuse optics exhaustively; rather, the aim is to provide a snapshot of recent diffuse optics–based efforts to noninvasively quantify oxygen metabolism in breast tissue, with an emphasis (though not exclusively) on research from the authors' laboratories. For more extensive discussion on these issues, the reader is encouraged to peruse the primary articles cited, as well as recent reviews about diffuse optical imaging/spectroscopy[68,69] and diffuse correlation spectroscopy.[61,68,70–72]

The review is organized as follows. The initial focus is on the use of statistical analysis of diffuse optical data to derive a probability of malignancy for cancer localization and therapy tracking. The promise of diffuse optical data in metabolic

Table 1
Characteristics of several imaging modalities

	Radiography	PET	Ultrasonography	MR Imaging	Diffuse Optics
Ionizing radiation	Yes	Yes	No	No	No
Tissue structure	Yes	No	Yes	Yes	No
Tissue metabolism	No	Yes	No	No	Yes
Clinician's office	No	No	Yes	No	Yes
Frequent measurements	No	No	Yes	No	Yes

Note that diffuse optics permits convenient, nonionizing, and frequent measurement of tissue metabolism.

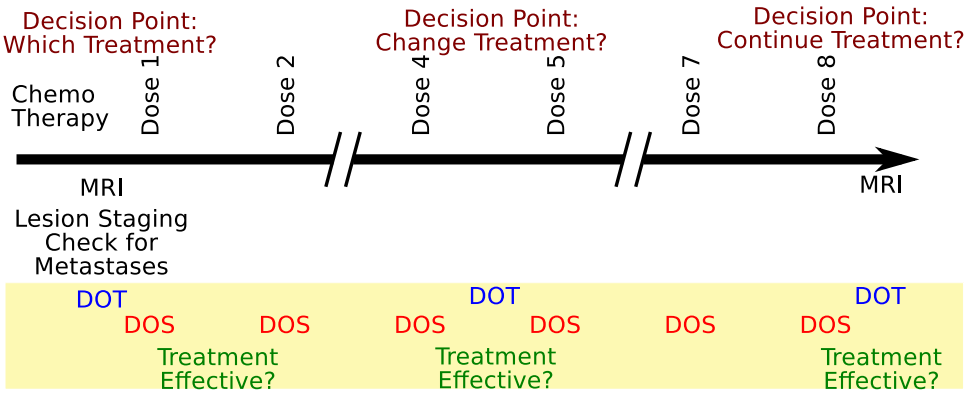

Fig. 1. A proposed timeline for including diffuse optical spectroscopy (DOS) and diffuse optical tomography (DOT) in the planning of neoadjuvant chemotherapy (*yellow box*). DOS provides rapid measurements, integrable into each patient visit. More time-consuming volumetric imaging with DOT provides more detailed information. Together, these frequent measurements of tissue metabolic state may permit clinicians to more rapidly shift to more efficacious treatment regimens or even identify a complete response before completion of all scheduled doses.

imaging is then examined. This is followed by a comparison study between endogenous DOT and FDG PET imaging, an all-optical metabolism measurement, and the use of external perturbations to probe tissue metabolism. Finally, the use of exogenous contrast agents in optical breast cancer imaging is reviewed.

THE PROPAGATION OF PHOTONS IN TISSUES
Physics of Diffuse Optics

Light in the Near Infra Red (NIR) spectral window (650–950 nm) is weakly absorbed but strongly scattered by tissue. **Fig. 2** depicts this scenario in a model turbid medium. **Fig. 2**B shows the propagation of laser light through a clear, non-scattering medium (tap water). Note that the light propagates straight across the bath, with minimal dispersion of the columnated beam. Scatterers are then added to the medium; with a small amount of scattering agent, the beam is broadened in a manner akin to the visibility on a "foggy day" (see **Fig. 2**C), and with a large amount of scattering agent the photon transport is diffusive as is NIR light in tissue (see **Fig. 2**D). Two length scales are important: (1) a photon random walk step (l^*) and (2) a photon absorption length (l_a). The random walk step (l^*), or photon transport mean free path, corresponds to the typical distance traveled by a typical photon before its initial propagation direction becomes randomized ($l^* \sim 1$ mm). For example, most of the photons shown in **Fig. 2**D have had their initial direction randomized, and the directionality of the laser

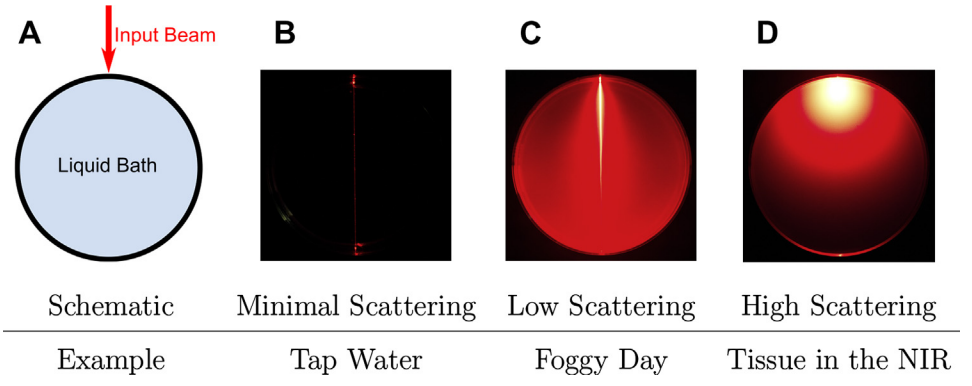

Fig. 2. Illustration of photon migration in turbid media. (*A*) A schematic of the experiment. (*B*) Container filled with tap water, with minimal scattering from air bubbles and tank walls. The columnated laser beam propagates straight across the liquid bath. (*C*) Container filled with a low scattering liquid (a dilute mixture of soy emulsion and water). The light beam is somewhat dispersed. (*D*) Container filled with a high scattering liquid (a more concentrated soy emulsion mixture). These optical properties are similar to tissue in the near-infrared (NIR) spectral region. Note that the light spreads almost isotropically from the point where the beam enters the scattering medium. Photos are in false color. (*Courtesy of* Han Ban, MS, University of Pennsylvania, Philadelphia, PA.)

beam is lost; by contrast, in **Fig. 2**C many photons are still traveling in a straight line through the medium. A wavelength (λ)-dependent reduced scattering coefficient $(\mu_s'(\lambda)=1/l)$ denotes the reciprocal of this photon transport mean free path, and is often the term of choice to describe tissue scattering. The absorption length (l_a) corresponds to the typical distance traveled by a photon before it is absorbed; it is also wavelength dependent. In the NIR range, this absorption length in tissue is typically much longer ($\sim$200 mm) than scattering length. Its reciprocal is denoted by the absorption coefficient ($\mu_a(\lambda)$).

The first incarnation of optical mammography in the 1920s[10,73] simply relied on the transmission of lamp light through the breast and its observation in a dark room. Unfortunately, as the authors of the original articles admit, this technique was highly qualitative and unreliable. In the early 1980s the technique was revisited, this time using wide-beam transillumination; however, it was not successful clinically, due (in part) to limited projection information and lack of separation of tissue absorption from tissue-scattering effects.[74–85]

The key to the reemergence of optical techniques for the imaging of breast cancer was the realization that light transport through tissue is a diffusive process and the subsequent development of accurate physical/mathematical models for photon propagation that separated tissue absorption from tissue-scattering effects. This mathematical approach enabled researchers to accurately quantify both tissue absorber (or chromophore) concentrations and tissue-scattering coefficients. By the mid-1990s the acceptance of this physical model, alongside the advances in the algorithms and technologies, reignited interest in the field.[86,87]

Once a paradigm was developed to separate tissue absorption from tissue scattering, the use of multiple optical wavelengths enabled experimenters to quantitatively determine the concentrations of various tissue chromophores (and contrast agents). For example, because oxyhemoglobin has an optical spectrum markedly different from that of deoxyhemoglobin (Hb) in the NIR (**Fig. 3**), it is readily possible to use absorption coefficient data at multiple wavelengths to recover absolute values of the concentrations of the hemoglobin species. Similar information about other chromophores, such as water and lipid content, and the scattering components of the tissue can be derived from the wavelength-dependent absorption and scattering data.

Fig. 4 illustrates two geometries frequently used in optical mammography. Parallel-plate transmission (left) and reemission (right) geometries for measurements are shown. Other geometries include rings, and combinations of transmission and reemission measurements. In all instruments, one or more light (e.g., laser) sources inject light into the tissue, and the light transmitted through

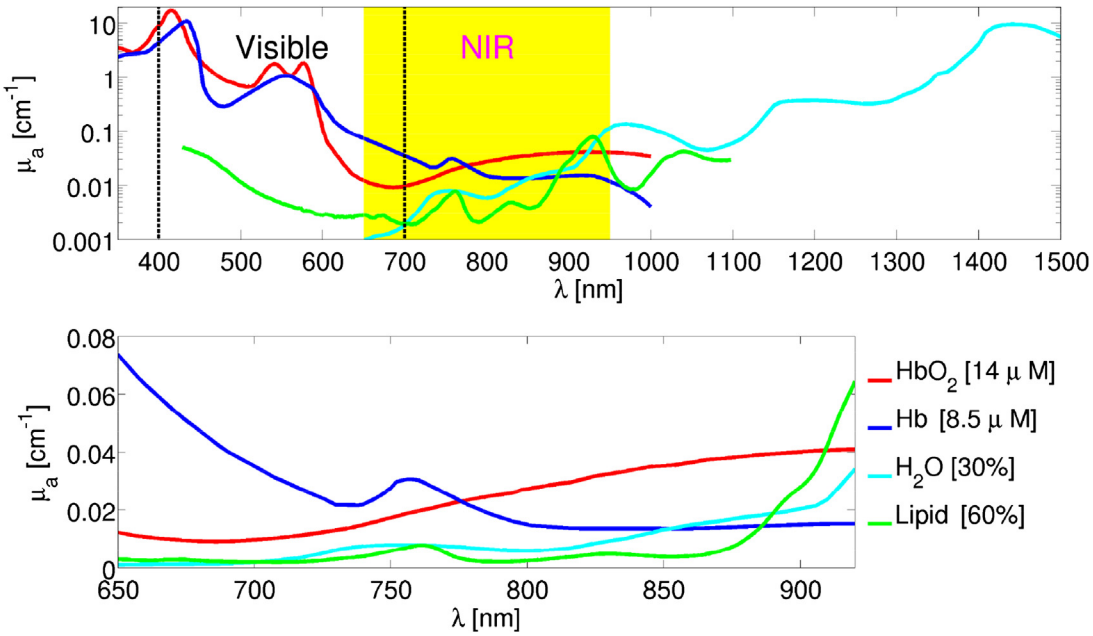

Fig. 3. Spectra of major tissue chromophores. (*Top*) the visible and NIR windows overlap somewhat; note the much lower absorption in the NIR. (*Bottom*) Expanded view of chromophores in the NIR spectral region at approximate concentrations found in human breast tissue.

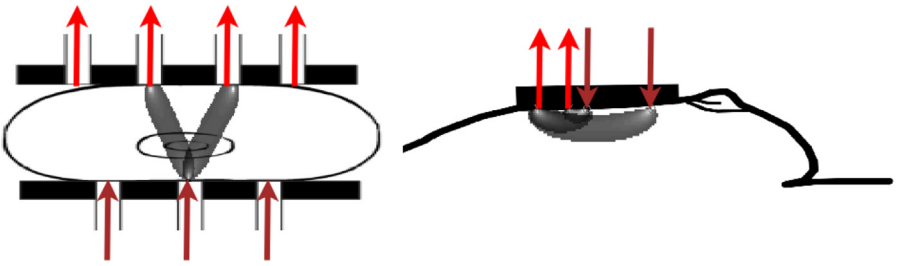

Fig. 4. Example transmission (*left*) and reemission (*right*) geometry measurements in optical mammography. One or more lasers typically inject light into the tissue (*maroon arrows*), and the light transmitted through the tissue is collected by one or more detectors (*red arrows*). Typical representations of the most probable trajectories of the detected photons are superimposed in gray scale.

the tissue is collected by one or more detectors. In **Fig. 4**, representations of the most probable trajectories of the detected photons are superimposed in gray scale; these trajectories are derived from analytical solutions of the photon diffusion equation in the relevant geometry.

PROBABILITY OF MALIGNANCY OPTICAL INDICES BASED ON DOT OF BREAST

Most current work in DOT focuses on the metabolically dependent physiologic variables, without explicitly calculating tissue metabolism. This section discusses DOT imaging of total hemoglobin concentration (Hb_t), blood oxygen saturation (StO_2), and tissue scattering (μ_s'), and the subsequent development of malignancy indices. Several researchers have pushed diffuse optical methods to add additional specificity for diagnosis; in some cases, this research has led to the development of useful combinations of the measured physiologic parameters or composite indices that better distinguish malignant from benign lesions.[13,35,51,88,89] Here the focus is on a recently developed computer-aided detection (CAD) technique that builds on ideas from the x-ray community to improve interpretation of radiologic data.[90] These CAD techniques are quite versatile; for example, besides use of multidimensional optical data, they permit simultaneous use of multiparameter data; for example, combining FDG uptake measured with PET and Gd contrast agent kinetics with MR imaging.[91]

DOT offers a fertile testing ground to apply these ideas in detection, diagnosis, and therapy monitoring of cancer. In general, each of the detected optical parameters is sensitive to tissue physiology, but interpretation of multiple 3D images is challenging. CAD offers a simple paradigm to develop composite indices, taking into account all parameters and their heterogeneities while deriving a single "probability of malignancy" tomogram. To date, several groups have applied statistical analysis techniques to multiparameter optical measurements to derive risk factors. Applications have included arthritic joints,[92] high-risk[93] or high-mammographic-density[23,24] breast tissue, and various "endoscopic" measurements or excised tissues.[94] However, these data sets have limited spatial information and orders of magnitude fewer measurements per subject than, for example, the breast tomograms to be discussed herein. Other researchers have implemented automated DOT image analysis techniques to identify lesions in a particular subject[95–97]; however, this analysis neglects information about the common signatures of cancer across a population.

Here the authors present illustrative results drawn from work conducted at the University of Pennsylvania.[35,66,98] The work is based on a set of 3D tomograms of total hemoglobin concentration (Hb_t), blood oxygen saturation (StO_2), and tissue scattering (μ_s') that were obtained from thirty five subjects with biopsy-confirmed lesions.[34,35] This data set permitted exploration of the potential of DOT-CAD for both cancer localization and the monitoring of cancer therapy.

The CAD algorithm requires identification of a group of subjects with data from both the modality under consideration (DOT) and a gold-standard diagnosis. Essentially, training-set data from this group is used to derive a common malignancy signature, from the combination of optical parameters that best reproduces the gold-standard diagnosis. As a test, the signature is then examined in additional subjects (the test set), who were not included in developing the diagnostic signature. Finally, the diagnostic results from the test set are compared with the gold-standard diagnosis to evaluate the utility of the test.

Regarding diffuse optical properties of breast, the authors[35] and others[20,51,99] have observed that the intersubject variation of physiologic parameters (Hb_t, StO_2, μ_s') can be quite large.

Therefore, the first technical strategy introduced was to adopt an intrasubject normalization scheme that reduces this intersubject variation. Specifically, all data are log-transformed, then the mean value of each parameter in healthy tissue for each subject is subtracted; finally, this result is divided by the standard deviation of the parameter in healthy tissue. Thus a "Z-score" normalized variable for each optical parameter is obtained. This *intrasubject* normalization spectacularly reduces the *intersubject* variation in all of the optically measured parameters, as shown in **Fig. 5**A.

With these new Z-score normalized tissue parameters one can sensibly combine the Hb_t, StO_2, and μ_s' data from the tissue volume elements (voxels) of multiple subjects (training set) to generate a single statistically derived malignancy parameter (M). M is a weighted linear combination of physiologic parameters from the training population of cancers. The weighting vectors, $\vec{\beta}$, are optimized using data from each voxel of each patient and logistic regression. The extracted weighting factors (or weighting vector) is then applied to an additional subject (test set); thus the M of each voxel in the subject is computed and a probability of malignancy ($P(M)$) for each volume element in the breast can be assigned. A threshold probability is then used to define a binary mask for cancer location (see **Fig. 5**B). Example results are shown in **Fig. 6**. Note that the blood oxygen saturation (StO_2) images (see **Fig. 6**B) have the least lesion contrast; the weighting factor of StO_2 is significantly smaller than Hb_t and μ_s'. Of interest, one of the authors' subjects with an *in situ* lesion (see **Fig. 6**, left column) exhibited a probability of malignancy that was significantly lower than the threshold cutoff obtained for malignant tissue. This observation suggests the potential for future versions of the metric to distinguish between types of lesions, as well as between healthy and malignant tissue.

The authors have recently extended the DOT-CAD results to monitor the efficacy of neoadjuvant chemotherapy.[66] The $P(M)$ calculation brings together several physiologic parameters to identify changes. In contrast to the composite probability of malignancy signature, significant differences were not observed in the responses of both absolute and relative values of the *individual* physiologic parameters (Hb_t, StO_2, μ_s'). Although this pilot study was limited to three subjects, two of whom responded completely to chemotherapy and one who had a partial response, the dynamics of changes in $P(M)$ between these two groups were significantly different (**Fig. 7**). The observations shown in **Figs. 6** and **7** demonstrate potential for extraction of a simple, clinically relevant metric for cancer staging and therapy monitoring from diffuse optical images. Promising early results[64] suggest that these optical techniques

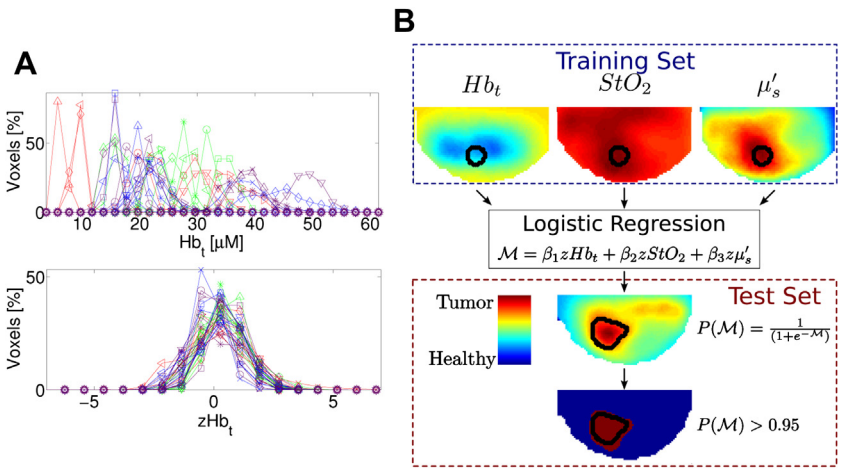

Fig. 5. (*A*) Intrasubject data normalization brings intersubject data distributions close to a normal distribution in the healthy tissue of thirty five breasts with biopsy-confirmed malignant lesions.[98] The top row shows, for the full population, absolute values of Hb_t, and the bottom row shows the population distribution of Z-transformed variables after intrasubject normalization (zHb_t). Each trace/color represents the healthy region of one subject. For clarity of presentation, the vertical axis is normalized to the total number of voxels in each subject. (*B*) Schematic of probability of malignancy calculation. Weighting coefficients $(\vec{\beta})$ are calculated from normalized data in a population of known cancers (training set); this same weighting vector is then applied to data from an additional subject (test set) to calculate a probability of malignancy ($P(M)$) and a binary mask of tumor location. (*From* Busch DR, Guo W, Choe R, et al. Computer aided automatic detection of malignant lesions in diffuse optical mammography. Med Phys 2010;37(4):1843; with permission.)

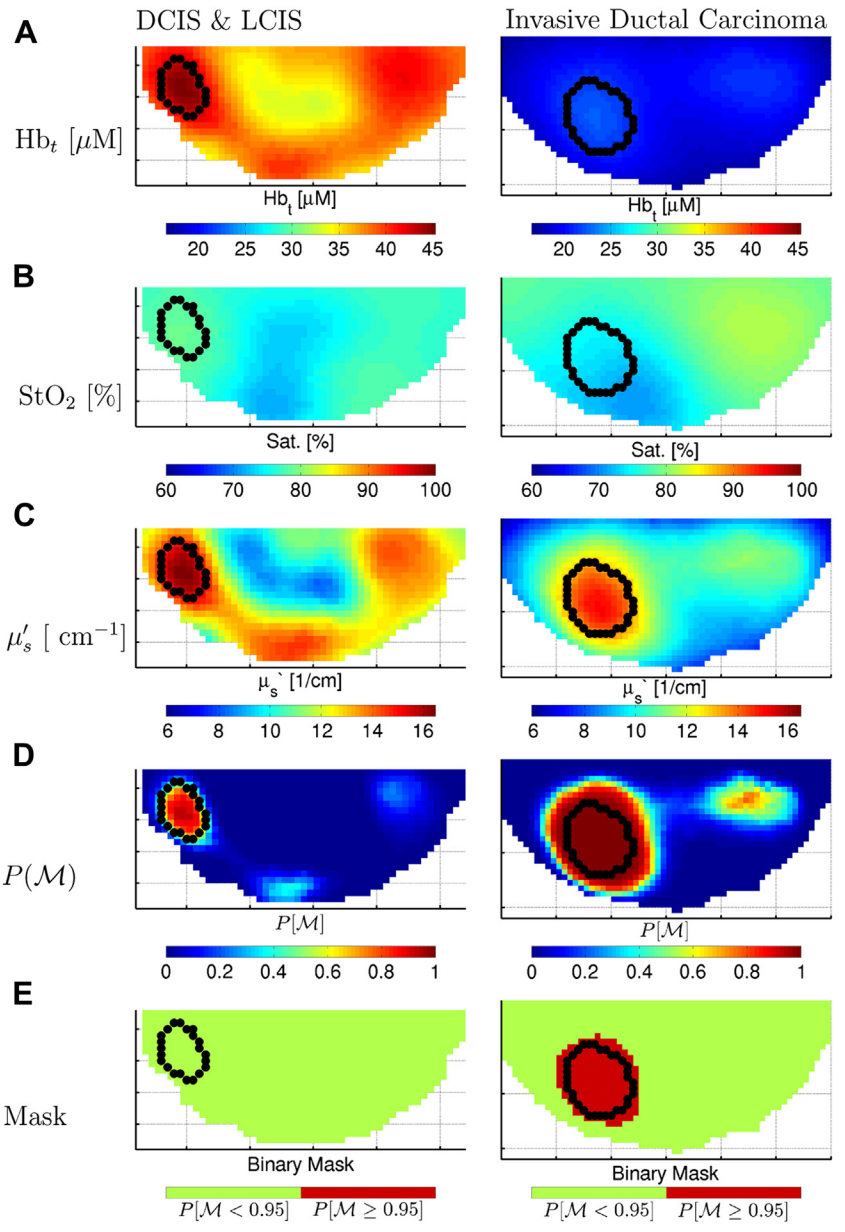

Fig. 6. Slices from three-dimensional (3D) images of two subjects, showing total hemoglobin concentration (*A*, Hb_t), blood oxygen saturation (*B*, StO_2), reduced scattering coefficient (*C*, μ_s'), probability of malignancy (*D*, $P(M)$), and a binary cancer mask (*E*) using a cutoff of $P(M) = 0.95$. The DCIS & LCIS (ductal and lobular carcinoma *in situ*) lesion in the left column provides an interesting case study, with the $P(M)$ falling between the malignant lesions and the healthy regions. The invasive ductal carcinoma in the right column shows a typical result from invasive cancers. (*From* Busch DR. Computer-aided, multi-modal, and compression diffuse optical studies of breast tissue [PhD thesis]. University of Pennsylvania; 2011; with permission.)

could be used to determine the efficacy of particular neoadjuvant chemotherapy regimens well before tumor changes are revealed by structural imaging.

Overall the results of this study are encouraging, suggesting that statistical analysis of the metabolically dependent, optically measured physiologic parameters of cancer tissue can yield a useful signature of cancer location and response to treatment. The study described here was derived from a limited population (thirty five subjects), and the chemotherapy monitoring is only at the pilot stage (three subjects). A more expansive study is now needed.

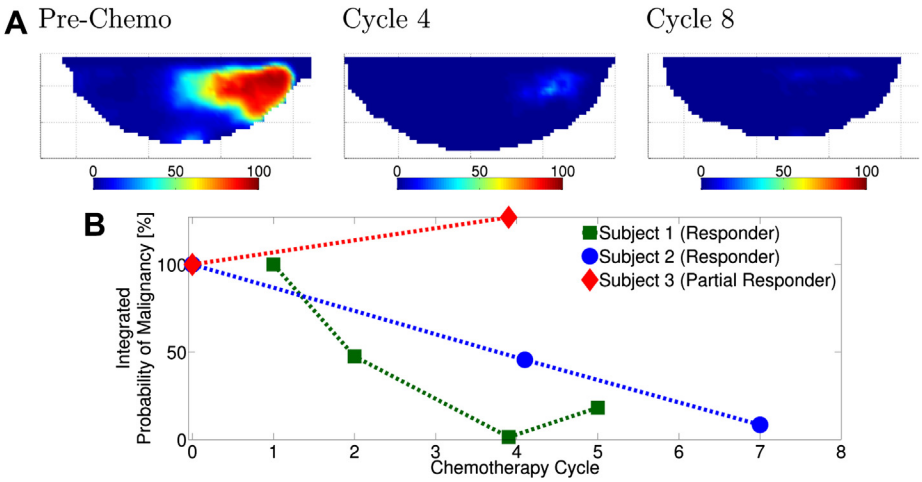

Fig. 7. Pilot study of monitoring chemotherapy using DOT with computer-aided detection in 3 subjects. (*A*) Example images of $P(M)$ changing during the course of chemotherapy (subject 2). (*B*) Integrated probability of malignancy in tumor regions, normalized to first time point in subjects with complete (subjects 1 and 2) and partial (subject 3) response to chemotherapy. (*From* Busch DR, Choe R, Rosen MA, et al. Optical malignancy parameters for monitoring progression of breast cancer neoadjuvant chemotherapy. Biomed Opt Express 2013;4(1):105–21.)

TOWARD METABOLIC IMAGING

Endogenous DOT Versus PET Glucose Imaging

It is difficult to validate the hemodynamic parameters measured by DOT directly against other diagnostic modalities, because none is able to noninvasively measure all of the same parameters. However, correlation of parameters such as the total hemoglobin concentration measured by DOT with microvessel density measured by histopathology has been carried out.[54,63,100,101] To date, two major approaches have been explored for direct correlation/comparison of DOT with other imaging modalities: (1) image correlation based on the stand-alone images taken independently, and (2) correlation based on concurrent image acquisition. The deformability of breast tissue makes the former approach challenging. Nonetheless, research along these lines has demonstrated that the high tumor-to-background ratio detected by DOT corresponds to the tumor locations identified by MR imaging[50,52,102] and PET.[89] These and other works have led to the development of advanced software suites that permit researchers to transform the volumetric information between imaging modalities.

Regarding concurrent acquisition, it is challenging but possible to integrate DOT source and detector systems into other medical imaging modalities. This development has led to interesting multimodal imaging instrumentation, for example, DOT and MR imaging,[103–106] DOT and tomosynthesis,[107,108] and, DOT and ultrasonographic imaging.[109–111] The primary disadvantage of the multimodal approach is that hardware constraints limit the total number of DOT measurements to values less than typical for stand-alone DOT systems. Most efforts to date have focused on use of anatomic information from MR imaging, tomosynthesis, and ultrasonography to derive spatial priors for DOT reconstructions; this concept has been shown to improve DOT quantification. Furthermore, concurrent multimodal imaging offers a great opportunity for DOT validation. In this vein, the combination of PET and DOT (and/or diffuse correlation spectroscopy) is interesting for validation of mechanisms of oxidative metabolism, and for consideration of DOT as a surrogate to PET when frequent measurements are desirable.

Although concurrent PET and DOT have not yet been demonstrated in humans, the coregistration and correlation of nonconcurrent DOT and PET has been performed.[89] **Fig. 8**A shows a qualitative correlation between FDG and DOT signals in axial, sagittal, and coronal views of patients' breasts. Note that PET imaged the whole body in this comparison, whereas DOT imaged a single breast. The dotted square in PET indicates the same breast imaged by DOT. Because image coregistration between breast images taken in supine and prone positions is difficult, each 3D image was analyzed independently for quantifying tumor-to-background ratio for each parameter. **Fig. 8**B shows a selected example from correlation between FDG and DOT-derived parameters. Positive correlations ($P<.05$) were found between FDG uptake and Hb_t, and FDG uptake and μ_s'. The positive correlation between FDG and Hb_t might be

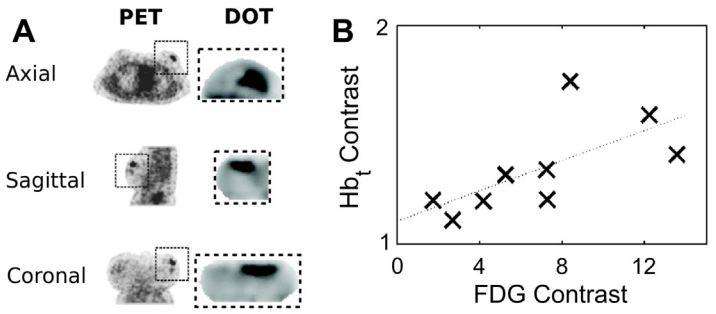

Fig. 8. (*A*) Axial, sagittal, and coronal slices from the whole-body FDG PET and DOT images of overall optical attenuation coefficient: μ_{eff}. Note the whole-body PET image is of the whole torso with both breasts, whereas DOT shows the left breast only. The rectangular dotted box in each image denotes the breast corresponding to the DOT image. (*B*) Correlation between contrast ratios in FDG uptake and Hb_t for the 9 patients with tumors visible to both DOT and PET. (*Adapted from* Konecky SD, Choe R, Corlu A, et al. Comparison of diffuse optical tomography of human breast with whole-body and breast-only positron emission tomography. Med Phys 2008;35(2):446–55; with permission.)

expected, because increases in glucose metabolism of breast cancer require more blood for glucose and oxygen delivery which, in turn, is typically accompanied by an increased total hemoglobin concentration.

For three patients, PET imaging was performed using a dedicated breast-imaging PET scanner.[112,113] Then, a coregistration algorithm based on rigid body motion (translation and rotation) and linear scaling[102] was used to transform the DOT image space into the PET image space as DOT was measured with axial compression whereas PET was measured without compression. A caudal-cranial slice from a 3D DOT image encompassing the suspicious mass for each parameter (Hb_t, StO_2, μ_s') is presented along with the FDG image slice in **Fig. 9**. Subject A had a ductal carcinoma *in situ*, subject B had a palpable mass that turned out to be a seroma caused by biopsy-induced hemorrhage in the center, and subject C had invasive ductal carcinoma. Increases in Hb_t and μ_s' contrast showed correspondence with similar high-FDG regions in the PET images. In sum, these results demonstrate that DOT is indeed sensitive to the local metabolism and may provide information complementary to PET.

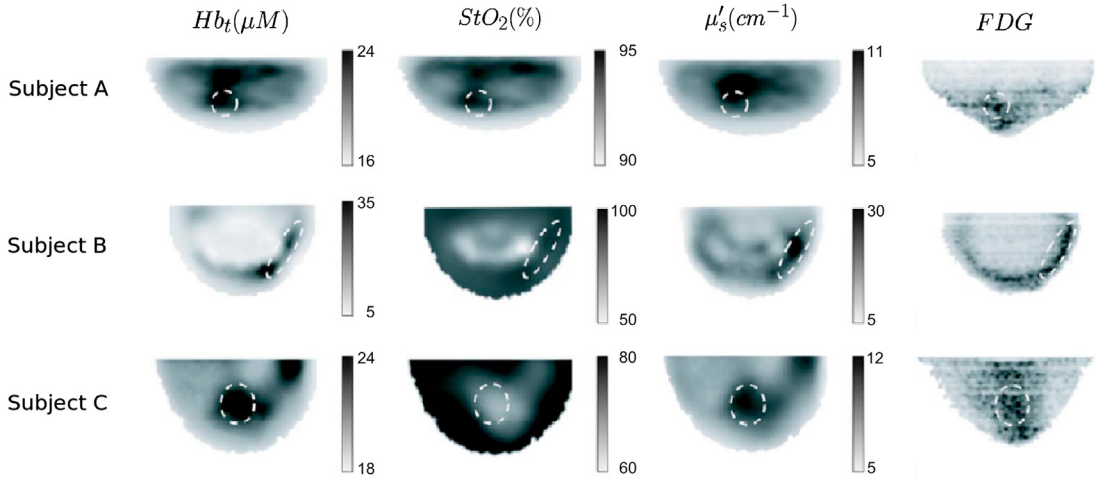

Fig. 9. Images of the breasts of three women imaged with DOT and with a dedicated breast-imaging PET. A representative caudal-cranial slice taken from the 3D reconstruction of a breast is presented for each parameter and patient. The DOT images have been transformed, using a coregistration algorithm, to be in the same uncompressed state as PET. The rows correspond to each patient with suspicious lesions. The columns correspond to Hb_t, StO_2, μ_s' measured by DOT, and FDG uptake measured by PET. The dashed white ellipses enclose regions with suspicious lesions. (*Adapted from* Konecky SD, Choe R, Corlu A, et al. Comparison of diffuse optical tomography of human breast with whole-body and breast-only positron emission tomography. Med Phys 2008;35(2):446–55; with permission.)

All-Optical Measurement of Oxygen Extraction Fraction and Metabolism

Another approach uses diffuse light to noninvasively measure microvascular, local blood flow (*BF*). The measurement uses a technique referred to as diffuse correlation spectroscopy (DCS) in the biomedical optics community.[61,68,114,115] DCS uses coherent laser sources and the temporal statistics of light speckles emerging from tissue. These statistics reveal quantitative information about the motion of red blood cells (RBCs) in the interrogated tissues. *BF* is characterized by an index derived from the temporal decay rate of the diffusing light field temporal intensity autocorrelation function.

Optical mammography, or breast tumor monitoring, with DCS was first introduced in 2005.[116] In that study, the investigators observed a significant increase of the DCS *BF* index in tumors in comparison with the normal tissue. Later, the investigators demonstrated that early changes in tumor physiology can also be discerned by DCS flow measurements and that the relative changes were comparable with relative changes measured by DOS/DOT.[53] Most recently, these approaches have shown potential to differentiate responders from nonresponders among patients on neoadjuvant chemotherapy, and potential for use in drug-development schemes.[61] For recent reviews, see Refs.[61,68]

DCS information can readily be combined with information from DOS/DOT to gain access to tissue oxygen metabolism. This combination is attractive for several reasons: (1) DCS and DOS/DOT probe very similar tissue volumes for the same source-detector positions, so the results are easily combined and compared; (2) the ability to collectively measure blood flow, blood volume, and blood oxygenation enables researchers to estimate the oxygen extraction fraction and the tissue metabolic rate of oxygen extraction.[53,68,117]

To illustrate this latter point, two composite "optical indices" are introduced, which indicate the tissue physiology. The tissue optical index (*TOI*) suggested by the Tromberg group at the University of California, Irvine is a multiparameter contrast function created to maximize both the contrast and the specificity of the optical measurement. *TOI* is defined as[13,51]

$$\mathrm{TOI} = \frac{\mathrm{Hb}\cdot\mathrm{H_2O}}{\mathrm{Lipid}}\cdot \tag{1}$$

TOI is empirically constructed from the concentrations of deoxyhemoglobin (*Hb*), water (H_2O), and lipids (*Lipid*). Increased *TOI* has been found to reflect a higher chance of tumor malignancy, and *TOI* is also related to metabolic activity, because increases in deoxyhemoglobin are often a symptom of unmet metabolic demand.

Inclusion of DCS in the arsenal of diffuse optical tools for optical mammography enables one to derive a direct estimate of tissue oxygen metabolism by combining information about blood flow (delivery of oxygen) with the chromophore concentration information such as blood oxygen saturation (ie, oxygen availability). This approach has most often been employed in neurologic applications with hybrid diffuse optics,[68] but these ideas are readily translated to other tissues, albeit without a robust validation. Here, a simple model and index is described, which offers a new means to define tumor contrast based on mammary metabolic rate of oxygen consumption ($MMRO_2$) following Zhou.[53,117] We define

$$\mathrm{MMRO_2} = \gamma\cdot\frac{\mathrm{Hb}}{\mathrm{Hb_t}}\cdot\mathrm{BF} \tag{2}$$

where $\gamma = \dfrac{Hb_v/Hb_{tv}}{Hb/Hb_t}$, the ratio of deoxyhemoglobin (*Hb*) to total hemoglobin (Hb_t) in the venous compartment (*v*) compared with the ratio of deoxyhemoglobin to total hemoglobin in the total vasculature. Here, the relative rates of oxygen metabolism between tumor ("*T*") and normal ("*N*") breast tissues $\left(rMMRO_{2(T/N)} = \dfrac{MMRO_{2(T)}}{MMRO_{2(N)}}\right)$ are defined as

$$\mathrm{rMMRO_{2(T/N)}} = \frac{\gamma_T}{\gamma_N}\cdot\frac{\mathrm{Hb_{(T)}}}{\mathrm{Hb_{(N)}}}\cdot\left(\frac{\mathrm{Hb_{t(T)}}}{\mathrm{Hb_{t(N)}}}\right)^{-1}\cdot\frac{\mathrm{BF_{(T)}}}{\mathrm{BF_{(N)}}} \tag{3}$$

$$= \frac{\gamma_T}{\gamma_N}\cdot\mathrm{rHb_{(T/N)}}\cdot\left(\mathrm{rHb_{t(T/N)}}\right)^{-1}\cdot\mathrm{rBF_{(T/N)}}. \tag{4}$$

In Eqn. 4, the relative values of a parameter between tumor and normal tissue are abbreviated as $rX_{(T/N)} = X_T/X_N$. If it is assumed that the ratio of γ_T/γ_N is unity and constant over time, Eqn. 4 reduces to

$$\mathrm{rMMRO_{2(T/N)}} = \frac{\mathrm{rHb_{(T/N)}}}{\mathrm{rHb_{t(T/N)}}}\cdot\mathrm{rBF_{(T/N)}} \tag{5}$$

or alternatively

$$\mathrm{rMMRO_{2(T/N)}} = \frac{1}{1}\frac{\mathrm{StO_{2(T)}}}{\mathrm{StO_{2(N)}}}\cdot\mathrm{rBF_{(T/N)}} \tag{6}$$

where StO_2 is the tissue oxygen saturation.

$rMMRO_{2(T/N)}$ is thus the relative oxygen extraction multiplied by the relative blood flow in the tumor compared with the normal tissue; that is, $MMRO_2$ relates the local blood flow and the local oxygen extraction fraction to each other in a manner that is presumably proportional to the

extraction of oxygen derived from the local oxygen metabolism. $rMMRO_{2(T/N)}$ is an attempt to quantify the tumor oxygen metabolism with respect to the healthy surrounding tissue.

Fig. 10 shows how one can use these data and these new indices in monitoring cancer therapy. **Fig. 10** shows data from a 45-year-old premenopausal woman undergoing neoadjuvant chemotherapy treatment for an invasive ductal carcinoma in the left breast.[53,117] The patient was treated with neoadjuvant chemotherapy delivered in multiple stages. The initial treatment stage consisted of doxorubicin and cyclophosphamide. Further details are provided by Zhou and colleagues.[53,117]

The data shown in **Fig. 10** indicate the richness of the parameters measurable with the hybrid diffuse optical instrumentation. Both hemodynamic and structural information about the tumor are assessed over time. These parameters all show varying degrees of change as the therapy progresses at a very early stage, that is, as early as three days after the start of the therapy. In particular, *BF* measured with DCS increased initially on day three after the start of therapy, and then decreased sharply and in a sustained manner during days four, five, and seven. This type of behavior, in response to therapy, was found again in later studies and was suggested to indicate therapy response.[61]

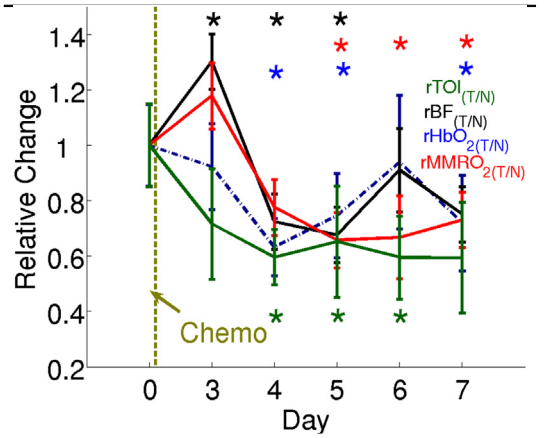

Fig. 10. Relative tumor/normal oxyhemoglobin ($rHbO_{2(T/N)}$), blood flow index ($rBF_{(T/N)}$), optical index ($rTOI_{(T/N)}$), and mammary metabolic rate of oxygen consumption ($rMMRO_{2(T/N)}$). Contrasts in response to chemotherapy are shown. The optical indices were calculated as the ratio of the average tumor value to the average value of the normal tissue on the same side of the breast. These indices were then normalized to the prechemotherapy values to reflect relative changes. Asterisk denotes statistically significant (at $P<.05$) difference from prechemotherapy values. (*Courtesy of* Chao Zhou, PhD, Lehigh University, Bethlehem, PA.)

Fig. 10 shows the evolution of the two composite indices $rMMRO_{2(T/N)}$ and $rTOI_{(T/N)}$ ($rTOI_{(T/N)} = TOI_T/TOI_N$). Note that they have diverged from one another by day three, wherein $rTOI_{(T/N)}$ showed an initial drop and $rMMRO_{2(T/N)}$ showed an initial increase. After day four, both metabolic indices dropped significantly and then stabilized until the end of the monitoring period. The authors of this work have speculated that although both $rTOI_{(T/N)}$ and $rMMRO_{2(T/N)}$ are related to tumor metabolic responses, $rTOI_{(T/N)}$ provides information about tumor cellular metabolic activities, whereas $rMMRO_{2(T/N)}$ provides information about tumor oxygen metabolic changes. At this time it is too early to say whether these composite parameters will prove to be useful in therapy monitoring or diagnostics in optical mammography, but they do provide a new approach to direct probing of the tissue physiology.

In principle, DCS can be used to carry out tomographic optical mammography of blood flow, that is, diffuse correlation tomography (DCT). At this time, however, DCT has only been demonstrated in tissue phantoms and in rat brain.[118] The authors expect that with increased parallelization and improved technologies, DCT might soon be used for breast imaging. In fact, some spectroscopic results in the transmission geometry have been published,[119] which suggest that with a better dynamic range it should be possible to construct a stand-alone breast DCT system.

Dynamic Imaging of Physiologic Perturbations

This section highlights a different approach to optical mammography, which uses physiologic perturbations to generate contrast in human breast tissue.[119–125] For example, internal or external applied pressure can alter tissue optical properties in a predictable manner, and thus provide the experimenter with additional metabolic/hemodynamic tissue information and contrast. Specifically, Carp and colleagues[126] have used mild cyclical perturbations of the applied load to derive an estimate for the baseline metabolism of breast tissue. Their experiment consisted of placing the breast between two parallel plates, similar to the geometry of an axial mammogram. Then frequency-domain optical data (DOS) was collected in the remission geometry from the inferior plate as a stepper motor applied force (up to 6 lb/2.7 kg) to the superior plate for ninty seconds (repeating the cycle three times). The underlying idea of this approach is that the changes in total hemoglobin concentration in response to partial

vessel occlusion serve as a proxy for net, bulk blood flow. This notion is essentially borrowed from other areas such as venous cuff-occlusion photoplethysmography. The derived flow information is combined with measured changes in tissue oxygen saturation, in a manner similar to the aforementioned $MMRO_2$, to calculate the bulk tissue oxygen consumption. When compared with values reported in the literature (**Table 2**), their measurements appear to underestimate these quantities. However, in the remission geometry one might also expect the measurements to be much more sensitive to the outer fatty region of breast rather than the central fibroglandular region. Thus, the underestimation may be due to low blood flow and oxygen consumption in the fatty region. Despite this limitation, this approach represents a step forward regarding extraction of absolute numbers for oxygen consumption and blood flow.

Similarly, while not explicitly extracting metabolic parameters, other scientists have used compression schemes to create differential images based on the variation of the compressibility and/or the vascular resistance of the tumors by comparison with surrounding healthy tissue.[17,38,120–122] Xu and colleagues[124] have developed a hand-held pressure modulation device, and Dixit and colleagues[129,130] have used inhaled gasses to generate vascular contrast.[131] Overall, these dynamic methods demonstrate the versatility of the diffuse optical techniques in seeking different physiologic contrasts.

EXOGENOUS CONTRAST AGENTS

Like other conventional imaging modalities, the capabilities of diffuse optics can be enhanced with the use of exogenous contrast agents. With the increase in contrast by use of a contrast agent, image resolution and fidelity can be improved. In a different vein and perhaps more interestingly, DOT could be used to access numerous parameters related to tumor pathology (e.g. pH, tumor-specific receptors, glucose metabolism) with optimized tumor-targeting optical contrast agents.[132] Such agents are commonly used in animal models, and are expected to become more widely available for human use in the near future.

At present, the metabolic sensitivity and the spatial resolution of DOT are analogous to that of PET before the advent of PET/computed tomography (CT) systems. As noted earlier, several research groups are exploring potential multimodal combinations of DOT with other techniques that are sensitive to tissue structure. This multimodal approach, analogous to that of PET/CT, could open a new chapter for the field. An interesting advantage to DOT, for example, in comparison with some modalities is its potential for simultaneous imaging of multiple contrast agents. This capability provides opportunities for simultaneous monitoring of several tumor characteristics.[106,133]

Indocyanine green (ICG, sold under the brand name Cardio-Green[134]) is currently the only agent approved by the Food and Drug Administration for use as an absorption-enhancing or a fluorescence agent in the NIR spectral region. In this case, the absorption/excitation (peak ~800 nm) and emission (peak ~820 nm) wavelengths have low absorption in tissue, permitting highly sensitive detection. ICG is used routinely in the clinic for measurement of cardiac output, in hepatology for evaluation of liver function, in ophthalmology for choroidal angiography, and in neurology for detection of cerebral artery infarction.[135] In plasma, rapid binding of ICG to macromolecules such as lipoproteins and albumin causes ICG to act as a blood-pooling agent. ICG is eliminated by the liver with a half-life of a few minutes.[136] In malignant tumors, new blood vessels tend to be hyperpermeable, enabling large molecules such as albumin to extravasate into the interstitium.[137] Thus, there is a good probability that ICG bound to macromolecules could leak out of vasculature and therefore serve as a marker for vascular permeability.

Table 2
Comparison of metabolic parameters (oxygen consumption and blood flow) reported in the PET literature and estimated using DOS

Method	Breast	*N*	Oxygen Consumption (μmol/100 mL/min)	Blood Flow (mL/100 mL/min)
PET, ^{15}O inhalation[127]	Normal	9	19.8	3.96
PET, ^{15}O inhalation[128]	Normal	20	N/A	5.6 1.4
DOS[126]	Healthy	28	1.9 1.3	2.8 1.7

PET literature included both tumor and normal breast values, but only normal values are presented in this table for comparison.

The first uses of ICG in diffuse optics were as an absorption and fluorescence contrast agent for optical mammography. With a concurrent MR imaging/DOT device, absorption enhancement due to ICG at 830 nm was used to highlight different degrees of enhancement in three cases: one with an invasive ductal carcinoma, one with fibroadenoma, and another with no disease.[103] The highest tumor-to-normal contrast was found in the invasive ductal carcinoma in 2D DOT, and its location was confirmed with simultaneous MR imaging.

The first 3D reconstruction of ICG **fluorescence** in human breast has since been demonstrated in three subjects with malignant breast tumors.[138] High ICG concentration was found in the same region, exhibiting high endogenous contrast (ie, Hb_t, μ_s'); the fluorescence concentration contrast even for this blood-pool agent was significantly higher than endogenous contrast based on absorption/scattering. Of note, the contrast enhancement attributable to ICG was even more dramatic in the heterogeneously dense breast than in the entirely fatty breast. In addition to static imaging, some attempts at differentiating benign from malignant tumors have been performed, based on the different pharmacokinetics of ICG-based absorption contrast. These results have been mixed and to date have only been investigated in a limited number of subjects.[139–142] The mixed results could be attributed to the fact that these measurements were taken within 10 minutes after bolus ICG injection when the signal was dominated by ICG contained in the blood, but not by ICG in the extravascular space.

Researchers at Physikalisch-Technische Bundesanstalt (PTB) and Charité Hospital in Berlin have imaged ICG in vascular and extravascular phases using a combination of ICG bolus injection and continuous infusion (**Fig. 11**).[143] The fluorescence-to-absorption ratio image taken during the extravascular phase showed enhancement corresponding to the location of an invasive ductal carcinoma. This lesion was detected using contrast-enhanced MR imaging but was not detected in an x-ray mammogram. In the case of fibroadenoma, fluorescence-to-absorption ratio images were similar to those of surrounding healthy tissue. Charité has extended this study to twenty women with twenty one breast lesions (eight benign and thirteen malignant lesions) yielding mean sensitivity of 92% and specificity of 75%. Compared with the approximately 100% sensitivity and 25% specificity of conventional mammography alone, this fluorescence technique demonstrated improvement in specificity.[144]

Recently, Bayer Schering Healthcare (Berlin, Germany) has attempted to translate a new NIR fluorescent optical contrast agent, Omocianine, to human use. Omocianine is an ICG derivative with a plasma half-life of approximately fifteen hours in humans and with superior quantum efficiency compared with ICG (ie, higher florescence). However, absorption and fluorescence measurements did not differentiate between benign and malignant tumors with this particular agent.[135,145]

In summary, several research groups have demonstrated that quantification of in vivo fluorescent dye concentration in breast is feasible in humans. One can simply enhance vascular contrast for DOT with bolus ICG during the vascular phase and/or access an additional parameter, vascular leakiness, with a carefully designed ICG injection protocol in the extravascular phase. The latter parameter may be an especially powerful tool to differentiate benign and malignant lesions. Although Omocianine failed to show improvement over ICG in imaging of breast cancer, other researchers have found multiple applications for ICG fluorescent imaging in translational research.[146] When new fluorescent dyes with higher quantum efficiency than ICG, or moieties targeting particular cellular markers, finally are transitioned into the clinic, the arsenal of optically available tumor characteristics will increase, and optical imaging and monitoring should emerge as a powerful tool.

SUMMARY AND OUTLOOK

This article discusses the recent trends in optical mammography as the field moves toward metabolic imaging and monitoring. The discussion is oriented toward diffuse optics technologies, with attention to composite signatures of malignancy, metabolic information from blood flow and hemoglobin concentration parameters, exogenous contrast agents, and dynamic contrast. Indeed, the American Cancer Society 2003 guidelines for the screening of breast cancer recognized diffuse optical mammography as a promising technology, worthy of future study.[147] Since these guidelines were published a decade ago the field has advanced significantly, with several studies incorporating larger patient populations.[20,33,148–150] Researchers have focused on niche applications, for example, monitoring of neoadjuvant chemotherapy,[61,151] with perhaps the most exciting recent development, in terms of its translation to routine clinical use, being an ongoing trial sponsored by the American College of Radiology Imaging Network (ACRIN), in which patients on neoadjuvant chemotherapy are enrolled in a seven-site trial with identical instrumentation (ACRIN 6691).

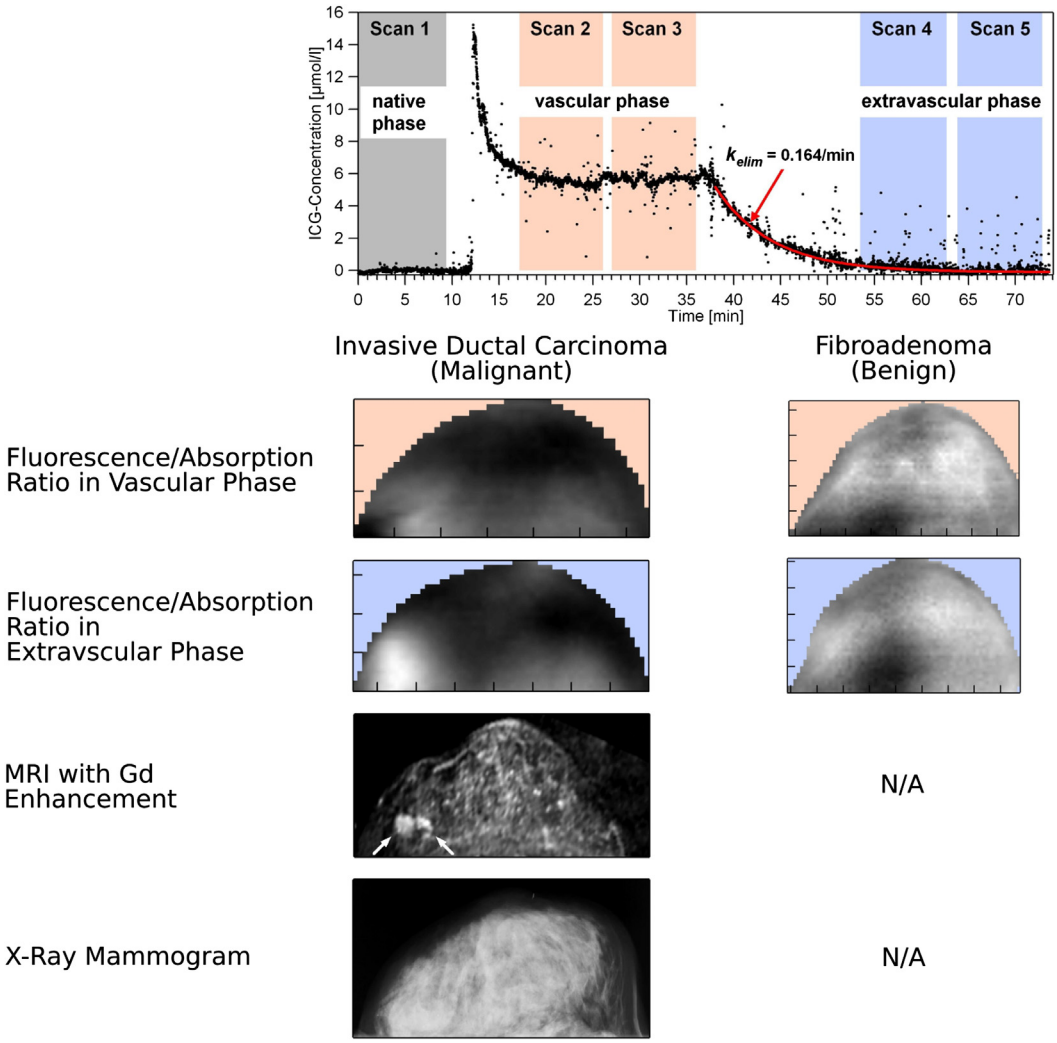

Fig. 11. (*Upper panel*) Time course of molar indocyanine green (ICG) concentration in arterial blood, recorded by transcutaneous pulse densitometry. Optical mammogram measurements were performed during the native phase (ie, before ICG injection, *gray shading*), vascular phase (ie, after ICG bolus injection followed by continuous infusion, *light salmon shading*), and extravascular phase (ie, more than 20 minutes after termination of infusion, *blue shading*). (*Lower panels*) Images of an invasive ductal carcinoma (malignant lesion, *center column*) and a fibroadenoma (benign lesion, *right column*). In the fluorescent/absorption ratio images, the malignant lesion lacks contrast in the vascular phase (*top row*), but is clearly visible in the extravascular phase (*second row*), whereas the benign lesion is much less distinct at both time points. Gadolinium-enhanced MR imaging (*third row*) shows the malignant lesion clearly, although this lesion is difficult to locate in the x-ray mammogram (*bottom row*).

In addition to the deep-tissue applications of diffuse optics, there has been considerable effort focused on intraoperative measurements of cancer margins and biopsy samples.[152–160] Fluorescence planar imaging through thin tissue for sentinel lymph nodes may also offer an alternative to radioscintigraphy.[161–163] Other notable recent developments not reviewed here include novel multimodal instrumentation combining diffuse optics with ultrasonography (photoacoustic tomography), taking advantage of hemoglobin absorption to selectively induce photothermal expansion. This rapid expansion produces a pressure wave detectable with ultrasound transducers,[164] a technique that has been demonstrated in the breast.[165–167]

It is hoped that the reader is able to discern that the diffuse optical technologies offer potential applications over a wide range of areas in the screening, detection, staging, and therapy monitoring of breast cancer. Indeed, in many ways

the present stage of DOT development parallels the early stages of PET. More advances need time for demonstration, but the outlook is exciting.

ACKNOWLEDGMENTS

The authors acknowledge fruitful collaborations and discussions about optics and clinical opportunities for optics over many years with numerous outstanding scientists including Britton Chance, Joseph P. Culver, Xingde Li, David A. Boas, Guoqiang Yu, Chao Zhou, Ulas Sunar, Bruce Tromberg, Rickson Mesquita, Mitchell D. Schnall, Mark A. Rosen, Brian J. Czerniecki, Julia Tchou, Douglas L. Fraker, Angela DeMichele, Carolyn Mies, Michael D. Feldman, Mary E. Putt, Wensheng Guo, Simon R. Arridge, Martin Schweiger, John C. Schotland, Alper Corlu, Soren D. Konecky, So Hyun Chung, Wesley Baker, Ashwin Parthasarathy, Kijoon Lee, Saurav Pathak, Han Y. Ban, Malavika Chandra, Yu Chen, Jonathan Fisher, Joe Giammarco, Monica Holboke, Xavier Intes, Xingde Li, Vasilis Ntziachristos, Maureen O'Leary, Yalin Ti, Hsing-Wen Wang, Guoqiang Yu, Udo Weigel, Peyman Zirak, Parisa Farzam, Johannes Johansson, Ki Won Jung, and Leonid Zubkov.

This research would not have been possible without the generosity of the research subjects who participated in the authors' studies.

REFERENCES

1. Siegel R, Naishadham D, Jemal A. Cancer statistics, 2012. CA Cancer J Clin 2012;62(1):10–29.
2. Kriege M, Brekelmans CT, Boetes C, et al. Efficacy of MRI and mammography for breast-cancer screening in women with a familial or genetic predisposition. N Engl J Med 2004;351(5):427–37.
3. Boyd J, Jellins J, Reeve T, et al. Ultrasound examination of the breast. In: Jellins J, Kobayashi T, editors. Doppler examination of the breast. New York: John Wiley and Sons; 1983. p. 385–6.
4. Sehgal CM, Weinstein SP, Arger PH, et al. A review of breast ultrasound. J Mammary Gland Biol Neoplasia 2006;11(2):113–23.
5. Saslow D, Boetes C, Burke W, et al. American Cancer Society guidelines for breast screening with MRI as an adjunct to mammography. CA Cancer J Clin 2007;57(2):75–89.
6. Lord S, Lei W, Craft P, et al. A systematic review of the effectiveness of magnetic resonance imaging (MRI) as an addition to mammography and ultrasound in screening young women at high risk of breast cancer. Eur J Cancer 2007;43(13):1905–17.
7. Weinstein SP, Localio AR, Conant EF, et al. Multimodality screening of high-risk women: a prospective cohort study. J Clin Oncol 2009;27(36):6124–8.
8. Rosen EL, Eubank WB, Mankoff DA. FDG PET, PET/CT, and breast cancer imaging. Radiographics 2007;27(Suppl 1):S215–29.
9. Wu WC, Englander S, Schnall, et al. Feasibility of arterial spin labeling in the measurement of breast perfusion. In: Proceedings of the International Society for Magnetic Resonance in Medicine. vol. 13. Berkeley, USA: International Society of Magnetic Resonance in Medicine; 2007. p. 2801.
10. Cutler M. Transillumination as an aid in the diagnosis of breast lesions. Surg Gynecol Obstet 1929;48:721–9.
11. Laser Institute of America. American national standard for the safe use of lasers: Ansi z136.1-2007. Orlando (FL): Laser Institute of America; 2007.
12. Food and Drug Administration. Code of federal regulations, title 21, vol. 8. US government Printing Office; 2003. 21CFR1040.10.
13. Cerussi A, Shah N, Hsiang D, et al. In vivo absorption, scattering, and physiologic properties of 58 malignant breast tumors determined by broadband diffuse optical spectroscopy. J Biomed Opt 2006;11:044005 (16pp).
14. Chance B, Nioka S, Zhang J, et al. Breast cancer detection based on incremental biochemical and physiological properties of breast cancers a six-year, two-site study. Acad Radiol 2005;12(8):925–33.
15. Durduran T, Choe R, Culver JP, et al. Bulk optical properties of healthy female breast tissue. Phys Med Biol 2002;47:2847–61.
16. Spinelli L, Torricelli A, Pifferi A, et al. Bulk optical properties and tissue components in the female breast from multiwavelength time-resolved optical mammography. J Biomed Opt 2004;9(6):1137–42.
17. Fang Q, Carp SA, Selb J, et al. Combined optical imaging and mammography of the healthy breast: optical contrast derived from breast structure and compression. IEEE Trans Med Imaging 2009;28(1):30–42.
18. Taroni P, Bassi A, Comelli D, et al. Diffuse optical spectroscopy of breast tissue extended to 1100 nm. J Biomed Opt 2009;14(5):054030.
19. Taroni P, Pifferi A, Salvagnini E, et al. Seven-wavelength time-resolved optical mammography extending beyond 1000 nm for breast collagen quantification. Opt Express 2009;17(18):15932–46.
20. Leff DR, Warren OJ, Enfield LC, et al. Diffuse optical imaging of the healthy and diseased breast: a systematic review. Breast Cancer Res Treat 2008;108(1):9–22.
21. Srinivasan S, Pogue BW, Carpenter C, et al. Developments in quantitative oxygen-saturation imaging of breast tissue in vivo using multispectral

near-infrared tomography. Antioxid Redox Signal 2007;9(8):1143–56.
22. Shah N, Cerussi AE, Jakubowski D, et al. Spatial variations in optical and physiological properties of healthy breast tissue. J Biomed Opt 2004;9(3): 534–40.
23. Blyschak K, Simick M, Jong R, et al. Classification of breast tissue density by optical transillumination spectroscopy: optical and physiological effects governing predictive value. Med Phys 2004;31(6): 1398–414.
24. Blackmore KM, Knight JA, Jong R, et al. Assessing breast tissue density by transillumination breast spectroscopy (TIBS): an intermediate indicator of cancer risk. Br J Radiol 2007;80(955):545–56.
25. Blackmore KM, Knight JA, Lilge L. Association between transillumination breast spectroscopy and quantitative mammographic features of the breast. Cancer Epidemiol Biomarkers Prev 2008;17(5): 1043.
26. Taroni P, Pifferi A, Quarto G, et al. Noninvasive assessment of breast cancer risk using time-resolved diffuse optical spectroscopy. J Biomed Opt 2010; 15:060501.
27. Nioka S, Chance B. NIR spectroscopic detection of breast cancer. Technol Cancer Res Treat 2005; 4(5):497–512.
28. Ntziachristos V, Chance B. Probing physiology and molecular function using optical imaging applications to breast cancer. Breast Cancer Res 2001;3: 41–6.
29. Enfield LC, Gibson AP, Everdell NL, et al. Three-dimensional time-resolved optical mammography of the uncompressed breast. Appl Opt 2007; 46(17):3628–38.
30. Poplack SP, Tosteson TD, Wells WA, et al. Electromagnetic breast imaging: results of a pilot study in women with abnormal mammograms. Radiology 2007;243(2):350–9.
31. Nioka S, Yung Y, Shnall M, et al. Optical imaging of breast tumor by means of continuous waves. Adv Exp Med Biol 1997;411:227–32.
32. Grosenick D, Wabnitz H, Rinneberg HH, et al. Development of a time-domain optical mammograph and first in vivo applications. Appl Opt 1999;38(13):2927–43.
33. Spinelli L, Torricelli A, Pifferi A, et al. Characterization of female breast lesions from multi-wavelength time-resolved optical mammography. Phys Med Biol 2005;50(11):2489–502.
34. Culver JP, Choe R, Holboke MJ, et al. Three-dimensional diffuse optical tomography in the parallel plane transmission geometry: evaluation of a hybrid frequency domain/continuous wave clinical system for breast imaging. Med Phys 2003;30:235–47.
35. Choe R, Konecky SD, Corlu A, et al. Differentiation of benign and malignant breast tumors by in-vivo three-dimensional parallel-plate diffuse optical tomography. J Biomed Opt 2009;14(2):024020 (18pp).
36. Hoogenraad JH, van der Mark MB, Colak SB, et al. First results from the Philips Optical Mammoscope. Photon Propagation in Tissues III 1998; 3194:184–90.
37. Nielsen T, Brendel B, Ziegler R, et al. Linear image reconstruction for a diffuse optical mammography system in a noncompressed geometry using scattering fluid. Appl Opt 2009;48(10):D1–13.
38. Schmitz CH, Klemer DP, Hardin R, et al. Design and implementation of dynamic near-infrared optical tomographic imaging instrumentation for simultaneous dual-breast measurements. Appl Opt 2005;44(11):2140–53.
39. Intes X, Djeziri S, Ichalalene Z, et al. Time-domain optical mammography Softscan: initial results. Acad Radiol 2005;12(8):934–47.
40. Athanasiou A, Vanel D, Fournier L, et al. Optical mammography: a new technique for visualizing breast lesions in women presenting non palpable BIRADS 4-5 imaging findings: preliminary results with radiologic-pathologic correlation. Cancer Imaging 2007;7(1):34.
41. Fournier LS, Vanel D, Athanasiou A, et al. Dynamic optical breast imaging: a novel technique to detect and characterize tumor vessels. Eur J Radiol 2009; 69(1):43–9.
42. Arridge S, Schotland J. Optical tomography: forward and inverse problems. Inverse Probl 2009; 25(12):123010 (59pp).
43. Kaufmann M, von Minckwitz G, Bear HD, et al. Recommendations from an international expert panel on the use of neoadjuvant (primary) systemic treatment of operable breast cancer: new perspectives 2006. Ann Oncol 2007;18(12):1927–34.
44. Arlinghaus LR, Li X, Levy M, et al. Current and future trends in magnetic resonance imaging assessments of the response of breast tumors to neoadjuvant chemotherapy. J Oncol 2010;2010. pii: 919620. 1–17.
45. Esserman L, Berry D, Cheang M, et al. Chemotherapy response and recurrence-free survival in neoadjuvant breast cancer depends on biomarker profiles: results from the I-SPY 1 TRIAL (CALGB 150007/150012; ACRIN 6657). Breast Cancer Res Treat 2011;30:3242–9.
46. McGuire K, Toro-Burguete J, Dang H, et al. MRI staging after neoadjuvant chemotherapy for breast cancer: does tumor biology affect accuracy? Ann Surg Oncol 2011;18(11):3149–54.
47. Falou O, Soliman H, Sadeghi-Naini A, et al. Diffuse optical spectroscopy evaluation of treatment response in women with locally advanced breast cancer receiving neoadjuvant chemotherapy. Transl Oncol 2012;5(4):238–46.

48. Tromberg BJ, Pogue BW, Paulsen KD, et al. Assessing the future of diffuse optical imaging technologies for breast cancer management. Med Phys 2008;35(6):2443–51.
49. Jakubowski DB, Cerussi AE, Bevilacqua F, et al. Monitoring neoadjuvant chemotherapy in breast cancer using quantitative diffuse optical spectroscopy: a case study. J Biomed Opt 2004;9(1):230–8.
50. Shah N, Gibbs J, Wolverton D, et al. Combined diffuse optical spectroscopy and contrast-enhanced magnetic resonance imaging for monitoring breast cancer neoadjuvant chemotherapy: a case study. J Biomed Opt 2005;10(5):051503.
51. Tromberg BJ, Cerussi A, Shah N, et al. Imaging in breast cancer: diffuse optics in breast cancer: detecting tumors in pre-menopausal women and monitoring neoadjuvant chemotherapy. Breast Cancer Res 2005;7(6):279–85.
52. Choe R, Corlu A, Lee K, et al. Diffuse optical tomography of breast cancer during neoadjuvant chemotherapy: a case study with comparison to MRI. Med Phys 2005;32:1128–39.
53. Zhou C, Choe R, Shah N, et al. Diffuse optical monitoring of blood flow and oxygenation in human breast cancer during early stages of neoadjuvant chemotherapy. J Biomed Opt 2007;12:051903.
54. Zhu Q, Tannenbaum S, Hegde P, et al. Noninvasive monitoring of breast cancer during neoadjuvant chemotherapy using optical tomography with ultrasound localization. Neoplasia 2008;10(10):1028–40.
55. Cerussi A, Hsiang D, Shah N, et al. Predicting response to breast cancer neoadjuvant chemotherapy using diffuse optical spectroscopy. Proc Natl Acad Sci U S A 2007;104(10):4014–9.
56. Tanamai W, Chen C, Siavoshi S, et al. Diffuse optical spectroscopy measurements of healing in breast tissue after core biopsy: case study. J Biomed Opt 2009;14(1):014024.
57. Jiang S, Pogue BW, Carpenter CM, et al. Evaluation of breast tumor response to neoadjuvant chemotherapy with tomographic diffuse optical spectroscopy: case studies of tumor region-of-interest changes. Radiology 2009;252:551–60.
58. Cerussi AE, Tanamai VW, Mehta RS, et al. Frequent optical imaging during breast cancer neoadjuvant chemotherapy reveals dynamic tumor physiology in an individual patient. Acad Radiol 2010;17(8):1031–9.
59. Soliman H, Gunasekara A, Rycroft M, et al. Functional imaging using diffuse optical spectroscopy of neoadjuvant chemotherapy response in women with locally advanced breast cancer. Clin Cancer Res 2010;16(9):2605–14.
60. Cerussi AE, Tanamai VW, Hsiang D, et al. Diffuse optical spectroscopic imaging correlates with final pathological response in breast cancer neoadjuvant chemotherapy. Philos Trans A Math Phys Eng Sci 2011;369(1955):4512–30.
61. Choe R, Durduran T. Diffuse optical monitoring of the neoadjuvant breast cancer therapy. IEEE J Sel Top Quantum Electron 2012;18(99):1367–86.
62. Enfield LC, Cantanhede G, Westbroek D, et al. Monitoring the response to primary medical therapy for breast cancer using three-dimensional time-resolved optical mammography. Technol Cancer Res Treat 2011;10(6):533–47.
63. Pakalniskis MG, Wells WA, Schwab MC, et al. Tumor angiogenesis change estimated by using diffuse optical spectroscopic tomography: demonstrated correlation in women undergoing neoadjuvant chemotherapy for invasive breast cancer? Radiology 2011;259(2):365–74.
64. Roblyer D, Ueda S, Cerussi A, et al. Optical imaging of breast cancer oxyhemoglobin flare correlates with neoadjuvant chemotherapy response one day after starting treatment. Proc Natl Acad Sci U S A 2011;108(35):14626–31.
65. Santoro Y, Leproux A, Cerussi A, et al. Breast cancer spatial heterogeneity in near-infrared spectra and the prediction of neoadjuvant chemotherapy response. J Biomed Opt 2011;16:097007.
66. Busch DR, Choe R, Rosen MA, et al. Optical malignancy parameters for monitoring progression of breast cancer neoadjuvant chemotherapy. Biomed Opt Express 2013;4(1):105–21.
67. Chung SH, Mehta R, Tromberg BJ, et al. Non-invasive measurement of deep tissue temperature changes caused by apoptosis during breast cancer neoadjuvant chemotherapy: a case study. J Innov Opt Health Sci 2011;4(4):361–72.
68. Durduran T, Choe R, Baker WB, et al. Diffuse optics for tissue monitoring and tomography. Rep Progr Phys 2010;73(7):076701.
69. Jacques SL, Pogue BW. Tutorial on diffuse light transport. J Biomed Opt 2008;13(4). 041302–1:19.
70. Mesquita R, Durduran T, Yu G, et al. Direct measurement of tissue blood flow and metabolism with diffuse optics. Philos Trans A Math Phys Eng Sci 2011;369(1955):4390–406.
71. Yu G. Near-infrared diffuse correlation spectroscopy in cancer diagnosis and therapy monitoring. J Biomed Opt 2012;17(1). 010901–19.
72. Yu G. Diffuse correlation spectroscopy (DCS): a diagnostic tool for assessing tissue blood flow in vascular-related diseases and therapies. Curr Med Imaging Rev 2012;8(3):194–210.
73. Cutler M. Transillumination of the breast. Ann Surg 1931;93(1):223–34.
74. Homer MJ. Breast imaging: pitfalls, controversies, and some practical thoughts. Radiol Clin North Am 1985;23:459–72.
75. Watmough DJ. Transillumination of breast tissues: factors governing optimal imaging of lesions. Radiology 1983;147:89–92.

76. Sickles EA. Breast cancer detection with transillumination and mammography. Am J Roentgenol 1984;142:841–4.
77. Wallberg H, Alveryd A, Bergvall U, et al. Diaphanography in breast carcinoma. Acta Radiol Diagn 1985;26:33–44.
78. Profio AE, Navarro GA. Scientific basis of breast diaphanography. Med Phys 1989;16:60–5.
79. Pera A, Freimanis AK. The choice of radiologic procedures in the diagnosis of breast disease. Obstet Gynecol Clin North Am 1987;14(3):635–50.
80. Carlsen EN. Transillumination light scanning. Diagn Imaging 1982;4:28–34.
81. Marshall V, Williams DC, Smith KD. Diaphanography as a means of detecting breast cancer. Radiology 1984;150:339–43.
82. Monsees B, Destouet JM, Totty WG. Light scanning versus mammography in breast cancer detection. Radiology 1987;163:463–5.
83. Gisvold JJ, Brown LR, Swee RG, et al. Comparison of mammography and transillumination light scanning in the detection of breast lesions. AJR Am J Roentgenol 1986;147(1):191–4.
84. Bartrum RJ Jr, Crow HC. Transillumination light scanning to diagnose breast cancer: a feasibility study. AJR Am J Roentgenol 1984;142:409–14.
85. Alveryd A, Andersson I, Aspegren K, et al. Lights canning versus mammography for the detection of breast cancer in screening and clinical practice. A Swedish multicenter study. Cancer 1990;65(8): 1671–7.
86. Hebden J, Arridge S, Delpy D. Optical imaging in medicine: I. Experimental techniques. Phys Med Biol 1997;42:825–40.
87. Arridge SR, Hebden JC. Optical imaging in medicine: II. Modelling and reconstruction. Phys Med Biol 1997;42(5):841–53.
88. Zhu Q, Hegde PU, Ricci A, et al. Early-stage invasive breast cancers: potential role of optical tomography with us localization in assisting diagnosis. Radiology 2010;256(2):367–78.
89. Konecky SD, Choe R, Corlu A, et al. Comparison of diffuse optical tomography of human breast with whole-body and breast-only positron emission tomography. Med Phys 2008;35(2):446–55.
90. Doi K. Computer-aided diagnosis in medical imaging: historical review, current status and future potential. Comput Med Imaging Graph 2007;31(4–5):198.
91. Pichler BJ, Kolb A, Nägele T, et al. PET/MRI: paving the way for the next generation of clinical multimodality imaging applications. J Nucl Med 2010; 51(3):333–6.
92. Klose CD, Klose AD, Netz U, et al. Multiparameter classifications of optical tomographic images. J Biomed Opt 2008;13(5):050503.
93. Simick MK, Jong R, Wilson B, et al. Non-ionizing near-infrared radiation transillumination spectroscopy for breast tissue density and assessment of breast cancer risk. J Biomed Opt 2004;9(4):794–803.
94. Zhu C, Breslin TM, Harter J, et al. Model based and empirical spectral analysis for the diagnosis of breast cancer. Opt Express 2008;16(19):14961–78.
95. Song X, Pogue BW, Jiang S, et al. Automated region detection based on the contrast-to-noise ratio in near-infrared tomography. Appl Opt 2004;43(5): 1053–62.
96. Pogue BW, Davis SC, Song X, et al. Image analysis methods for diffuse optical tomography. J Biomed Opt 2006;11(3):033001 (16pp).
97. Wang JZ, Liang X, Zhang Q, et al. Automated breast cancer classification using near-infrared optical tomographic images. J Biomed Opt 2008;13: 044001 (10pp).
98. Busch DR, Guo W, Choe R, et al. Computer aided automatic detection of malignant lesions in diffuse optical mammography. Med Phys 2010;37(4): 1840–9.
99. Pogue BW, Jiang S, Dehghani H, et al. Characterization of hemoglobin, water, and NIR scattering in breast tissue: analysis of intersubject variability and menstrual cycle changes. J Biomed Opt 2004;9:541.
100. Pogue BW, Poplack SP, McBride TO, et al. Quantitative hemoglobin tomography with diffuse near-infrared spectroscopy: pilot results in the breast. Radiology 2001;218(1):261.
101. Srinivasan S, Pogue BW, Brooksby B, et al. Near-infrared characterization of breast tumors in vivo using spectrally-constrained reconstruction. Technol Cancer Res Treat 2005;4(5):513–26.
102. Azar FS, Lee K, Khamene A, et al. Standardized platform for coregistration of nonconcurrent diffuse optical and magnetic resonance breast images obtained in different geometries. J Biomed Opt 2007; 12(5):051902.
103. Ntziachristos V, Yodh AG, Schnall M, et al. Concurrent MRI and diffuse optical tomography of breast after indocyanine green enhancement. Proc Natl Acad Sci U S A 2000;97:2767–72.
104. Ntziachristos V, Yodh AG, Schnall MD, et al. MRI-guided diffuse optical spectroscopy of malignant and benign breast lesions. Neoplasia 2002;4:347–54.
105. Carpenter CM, Srinivasan S, Pogue BW, et al. Methodology development for three-dimensional MR-guided near infrared spectroscopy of breast tumors. Opt Express 2008;16(22):17903–14.
106. Pogue BW, Leblond F, Krishnaswamy V, et al. Radiologic and near-infrared/optical spectroscopic imaging: where is the synergy? AJR Am J Roentgenol 2010;195:321–32.
107. Li A, Miller EL, Kilmer ME, et al. Tomographic optical breast imaging guided by three-dimensional mammography, guided by three-dimensional mammography. Appl Opt 2003;42(25):5181–90.

108. Boverman G, Miller EL, Li A, et al. Quantitative spectroscopic diffuse optical tomography of the breast guided by imperfect a priori structural information. Phys Med Biol 2005;50(17): 3941–56.
109. Zhu Q, Durduran T, Ntziachristos V, et al. Imager that combines near-infrared diffusive light and ultrasound. Opt Lett 1999;24:1050–2.
110. Holboke MJ, Tromberg BJ, Li X, et al. Three-dimensional diffuse optical mammography with ultrasound localization in a human subject. J Biomed Opt 2000;5:237–47.
111. Zhu Q, Tannenbaum S, Kurtzman SH. Optical tomography with ultrasound localization for breast cancer diagnosis and treatment monitoring. Surg Oncol Clin N Am 2007;16:307–21.
112. Freifelder R, Karp JS. Dedicated PET scanners for breast imaging. Phys Med Biol 1997;42: 2453–80.
113. Freifelder R, Cardi C, Grigoras I, et al. First results of a dedicated breast PET imager, BPET, using NaI(TI) curve plate detectors. IEEE Nucl Sci Symp Conf Rec 2001;3:1241–5.
114. Boas DA, Campbell LE, Yodh AG. Scattering and imaging with diffusing temporal field correlations. Phys Rev Lett 1995;75(9):1855–8.
115. Boas DA, Yodh AG. Spatially varying dynamical properties of turbid media probed with diffusing temporal light correlation. J Opt Soc Am A Opt Image Sci Vis 1997;14(1):192–215.
116. Durduran T, Choe R, Yu GQ, et al. Diffuse optical measurement of blood flow in breast tumors. Opt Lett 2005;30:2915–7.
117. Zhou C. In-vivo optical imaging and spectroscopy of cerebral hemodynamics [PhD thesis]. Philadelphia: University of Pennsylvania; 2007.
118. Zhou C, Yu G, Daisuke F, et al. Diffuse optical correlation tomography of cerebral blood flow during cortical spreading depression in rat brain. Opt Express 2006;14:1125–44.
119. Busch DR. Computer-aided, multi-modal, and compression diffuse optical studies of breast tissue [PhD thesis]. University of Pennsylvania; 2011.
120. Flexman M, Khalil M, Al Abdi R, et al. Digital optical tomography system for dynamic breast imaging. J Biomed Opt 2011;16:076014.
121. Al abdi R, Graber HL, Xu Y, et al. Optomechanical imaging system for breast cancer detection. J Opt Soc Am A Opt Image Sci Vis 2011;28(12):2473–93.
122. Jiang S, Pogue BW, Paulsen KD, et al. In vivo near-infrared spectral detection of pressure-induced changes in breast tissue. Opt Lett 2003;28(14): 1212–4.
123. Jiang SD, Pogue BW, Laughney AM. Measurement of pressure-displacement kinetics of hemoglobin in normal breast tissue with near-infrared spectral imaging. Appl Opt 2009;48(10).
124. Xu RX, Qiang B, Mao JJ, et al. Development of a handheld near-infrared imager for dynamic characterization of in vivo biological tissue systems. Appl Opt 2007;46(30):7442–51.
125. Carp SA, Kauffman T, Fang Q, et al. Compression-induced changes in the physiological state of the breast as observed through frequency domain photon migration measurements. J Biomed Opt 2006;11(6):064016.
126. Carp SA, Selb J, Fang Q, et al. Dynamic functional and mechanical response of breast tissue to compression. Opt Express 2008;16(20):16064–78.
127. Beaney RP, Lammertsma AA, Jones T, et al. Positron emission tomography for in-vivo measurement of regional blood flow, oxygen utilisation, and blood volume in patients with breast carcinoma. Lancet 1984;1:131–4.
128. Wilson CB, Lammertsma AA, McKenzie CG, et al. Measurements of blood flow and exchanging water space in breast tumors using positron emission tomography: a rapid and noninvasive dynamic method. Cancer Res 1992;52:1592–7.
129. Dixit SS, Kim H, Comstock C, et al. Near infrared transillumination imaging of breast cancer with vasoactive inhalation contrast. Biomed Opt Express 2010;1(1):295–309.
130. Dixit SS, Kim H, Visser B, et al. Development of a transillumination infrared modality for differential vasoactive optical imaging. Appl Opt 2009;48:100949.
131. Kotz KT, Dixit SS, Gibbs AD, et al. Inspiratory contrast for in vivo optical imaging. Opt Express 2008;16(1):19–31.
132. Weissleder R, Ntziachristos V. Shedding light onto live molecular targets. Nat Med 2003;9(1):123–8.
133. Tichauer KM, Holt RW, El-Ghussein F, et al. Dual-tracer background subtraction approach for fluorescent molecular tomography. J Biomed Opt 2013;18(1):16003.
134. Akorn Inc. IC-Green™ Sterile Indocyanine Green [Drug Packaging Insert]. Version: 6-DCGN-01 2006.
135. Poellinger A. Near-infrared imaging of breast cancer using optical contrast agents. J Biophotonics 2012;5(11–12):815–26.
136. Ott P. Hepatic elimination of indocyanine green with special reference to distribution kinetics and the influence of plasma protein binding. Pharmacol Toxicol 1998;83(S2):1–48.
137. Carmeliet P, Jain RK. Angiogenesis in cancer and other diseases. Nature 2000;407:249–57.
138. Corlu A, Choe R, Durduran T, et al. Three-dimensional in vivo fluorescence diffuse optical tomography of breast cancer in humans. Opt Express 2007;15(11):6696–716.
139. Intes X, Ripoll J, Chen Y, et al. In vivo continuous-wave optical breast imaging enhanced with indocyanine green. Med Phys 2003;30(6):1039–47.

140. Alacam B, Yazici B, Intes X, et al. Pharmacokinetic-rate images of indocyanine green for breast tumors using near-infrared optical methods. Phys Med Biol 2008;53:837–59.
141. Rinneberg H, Grosenick D, Moesta KT, et al. Detection and characterization of breast tumours by time-domain scanning optical mammography. Opto-Electronics Review 2008;16(2):147–62.
142. Schneider P, Piper S, Schmitz CH, et al. Fast 3D near-infrared breast imaging using indocyanine green for detection and characterization of breast lesions. Rofo 2011;183(10):956–63.
143. Hagen A, Grosenick D, Macdonald R, et al. Late-fluorescence mammography assesses tumor capillary permeability and differentiates malignant from benign lesions. Opt Express 2009;17(19):17016–33.
144. Poellinger A, Burock S, Grosenick D, et al. Breast cancer: early- and late-fluorescence near-infrared imaging with indocyanine green—preliminary study. Radiology 2011;258(2):409.
145. Poellinger A, Persigehl T, Mahler M, et al. Near-infrared imaging of the breast using omocianine as a fluorescent dye: results of a placebo-controlled, clinical, multicenter trial. Invest Radiol 2011;46(11):697–704.
146. Sevick-Muraca E. Translation of near-infrared fluorescence imaging technologies: emerging clinical applications. Annu Rev Med 2012;63:217–31.
147. Smith RA, Saslow D, Sawyer KA, et al. American Cancer Society guidelines for breast cancer screening: update 2003. CA Cancer J Clin 2003; 53(3):141–69.
148. Grosenick D, Wabnitz H, Moesta KT, et al. Time-domain scanning optical mammography: II. Optical properties and tissue parameters of 87 carcinomas. Phys Med Biol 2005;50(11): 2451–68.
149. Grosenick D, Moesta KT, Mller M, et al. Time-domain scanning optical mammography: I. Recording and assessment of mammograms of 154 patients. Phys Med Biol 2005;50(11):2429–49.
150. Taroni P, Danesini G, Torricelli A, et al. Clinical trial of time-resolved scanning optical mammography at 4 wavelengths between 683 and 975 nm. J Biomed Opt 2004;9(3):464–73.
151. Enfield LC, Gibson AP, Hebden JC, et al. Optical tomography of breast cancer-monitoring response to primary medical therapy. Target Oncol 2009;4: 219–33.
152. Bigio IJ, Brown SG, Briggs G, et al. Diagnosis of breast cancer using elastic-scattering spectroscopy: preliminary clinical results. J Biomed Opt 2000;5:221–8.
153. Keller MD, Majumder SK, Mahadevan-Lansen A. Spatially offset Raman spectroscopy of layered soft tissues. Opt Lett 2009;34:926–8.
154. Haka AS, Volynskaya Z, Gardecki JA, et al. Diagnosing breast cancer using Raman spectroscopy: prospective analysis. J Biomed Opt 2009;14: 054023.
155. Nguyen FT, Zysk AM, Chaney EJ, et al. Intraoperative evaluation of breast tumor margins with optical coherence tomography. Cancer Res 2009;69: 8790–6.
156. Nachabé R, Evers DJ, Hendriks BH, et al. Diagnosis of breast cancer using diffuse optical spectroscopy from 500 to 1600 nm: comparison of classification methods. J Biomed Opt 2011;16:087010.
157. Wilke LG, Brown JQ, Bydlon TM, et al. Rapid noninvasive optical imaging of tissue composition in breast tumor margins. Am J Surg 2009;198:566–74.
158. Brown JQ, Bydlon TM, Richards LM, et al. Optical assessment of tumor resection margins in the breast. IEEE J Sel Top Quantum Electron 2010; 16(3):530–44.
159. Bydlon TM, Barry WT, Kennedy SA, et al. Advancing optical imaging for breast margin assessment: an analysis of excisional time, cautery, and patent blue dye on underlying sources of contrast. PLoS One 2012;7:e51418.
160. McLaughlin RA, Quirk BC, Kirk RW, et al. Imaging of breast cancer with optical coherence tomography needle probes: feasibility and initial results. IEEE J Sel Top Quantum Electron 2012; 18:1184–91.
161. Tanaka E, Choi HS, Fujii H, et al. Image-guided oncologic surgery using invisible light: completed pre-clinical development for sentinel lymph node mapping. Ann Surg Oncol 2006;13:1671–81.
162. Sevick-Muraca EM, Sharma R, Rasmussen JC, et al. Imaging of lymph flow in breast cancer patients after microdose administration of a near-infrared fluorophore: feasibility study. Radiology 2008;246(3):734–41.
163. Hutteman M, Mieog JS, van der Vorst JR, et al. Randomized, double-blind comparison of indocyanine green with or without albumin premixing for near-infrared fluorescence imaging of sentinel lymph nodes in breast cancer patients. Breast Cancer Res Treat 2011;127(1):163–70.
164. Li C, Wang LV. Photoacoustic tomography and sensing in biomedicine. Phys Med Biol 2009; 54(19):R59.
165. Oraevsky AA, Jacques SL, Tittel FK. Measurement of tissue optical properties by time-resolved detection of laser-induced transient stress. Appl Opt 1997;36(1):402–15.
166. Ermilov SA, Khamapirad T, Conjusteau A, et al. Laser optoacoustic imaging system for detection of breast cancer. J Biomed Opt 2009;14(2):024007.
167. Kruger RA, Lam RB, Reinecke DR, et al. Photoacoustic angiography of the breast. Med Phys 2010;37(11):6096.